Quasi-analytical resolution-correction of elastic neutron scattering from proteins

Abir N. Hassani[1,2,3], Andreas M. Stadler[3,4] *, and Gerald R. Kneller[1,2†]

[1]*Centre de Biophysique Moléculaire, CNRS and Univ. d'Orléans; Rue Charles Sadron, 45071 Orléans, France*
[2]*Synchrotron Soleil; L'Orme de Merisiers, 91192 Gif-sur-Yvette, France*
[3]*Jülich Centre for Neutron Science (JCNS-1) and Institute of Biological Information Processing (IBI-8),*
Forschungszentrum Jülich GmbH, 52425 Jülich, Germany, and
[4] *Institute of Physical Chemistry, RWTH Aachen University, Landoltweg 2, 52056 Aachen, Germany*

Elastic neutron scattering from proteins reflects the motional amplitudes resulting from their internal collective and single-atom dynamics and is observable if the global diffusion of whole molecules is either blocked or cannot be resolved by the spectrometer under consideration. Due to finite instrumental resolution the measured elastic scattering amplitude always contains contaminations from quasielastic neutron scattering and some model must be assumed to extract the resolution-corrected counterpart from corresponding experimental spectra. Here we derive a quasi-analytical method for that purpose, assuming hat the intermediate scattering function relaxes with a "stretched" Mittag-Leffler function, $E_\alpha(-(t/\tau)^\alpha)$ $(0 < \alpha < 1)$, towards the elastic amplitude and that the instrumental resolution function has Gaussian form. The corresponding function can be integrated into into a fitting procedure and allows for eliminating the elastic intensity as a fit parameter. We illustrate the method for the analysis of two proteins in solution, the intrinsically disordered Myelin Basic Protein, confirming recently published results [J. Chem. Phys. 156(2):025102 (2022)], and the well-folded globular protein myoglobin. We also briefly discuss the consequences of our findings for the extraction of mean square position fluctuations from elastic scans.

I. INTRODUCTION

Thermal neutron scattering is a powerful and versatile spectroscopic method to probe the structural dynamics of condensed matter systems.[1] An important application concerns quasielastic neutron scattering (QENS) from proteins, which gives information about the diffusion and the relaxation dynamics of these macromolecules.[2–6] To probe the internal non-exponential multiscale relaxation dynamics, which is crucial for their function and typical for complex systems in general,[7–10] one can either use hydrated powder samples, where global diffusional motions are simply blocked, or probe a protein solution with a spectrometer that will not resolve these motions. In both cases, information about the motional amplitudes of internal protein dynamics is contained in the elastic amplitude and elastic scans are thus in principle sufficient to obtain this information. One must, however, be aware that the extracted motional amplitudes are underestimated due to the unavoidable contamination of the elastic amplitude by contributions from quasielastic scattering, and this correction can be particularly important for slowly relaxing systems.[11] Noting that the "true" elastic amplitude defines the asymptotic form of the neutron intermediate scattering function at infinite time, it can only be obtained by assuming some model for that function. A corresponding "minimalistic" model has been recently proposed and motivated in Ref. [12] and was then applied in a few subsequent QENS studies of protein dynamics,[13–15] as well as for confined water molecules in clays.[16] In all these studies the elastic amplitude was a fit parameter, which left some ambiguity about the physical significance of the resulting fits, in particular since the fit parameters are quite interdependent. The goal of this paper is to replace the elastic intensity as a fit parameter by an estimation on the basis of its experimentally measured counter part, the assumed model for the relaxation function, and the resolution of the instrument under consideration. Computational efficiency is here a fundamental aspect since it enables the integration of the corresponding function into the fitting procedure for the remaining parameters of the relaxation function.

The paper is organized as follows: The core of the paper is contained in the following Section II, which describes the theoretical background and the method, followed by Section IV showing some applications, and the Conclusions in Section V.

II. THEORETICAL BACKGROUND

A. Scattering functions

In standard neutron scattering experiments one measures the dynamic structure factor,

$$\tilde{F}(\mathbf{q}, \omega) = \frac{1}{2\pi} \int_{-\infty}^{+\infty} dt\, e^{-i\omega t} F(\mathbf{q}, t), \quad (1)$$

which is the time Fourier transform of the intermediate scattering function containing the information about the structural dynamics of the system under consideration,

$$F(\mathbf{q}, t) = \frac{1}{N} \sum_{j,k} \Gamma_{jk} \left\langle e^{-i\mathbf{q}\cdot\hat{\mathbf{R}}_j(0)} e^{i\mathbf{q}\cdot\hat{\mathbf{R}}_k(t)} \right\rangle. \quad (2)$$

*E-mail: a.stadler@fz-juelich.de
†E-mail: gerald.kneller@cnrs.fr

Usually the dynamic structure factor is denoted by $S(\mathbf{q},\omega)$, but we use the symbol $\tilde{F}(\mathbf{q},\omega)$ to label Fourier transforms in a uniform way. The scattering-related quantities are, respectively, the momentum and energy transfer from the neutron to the sample, $\mathbf{q}$ and ω, in units of $\hbar$, N is the total number of atoms in the scattering system and for each pair $\{j,k\}$ of them, $\{\hat{\mathbf{R}}_j(t),\hat{\mathbf{R}}_k(t)\}$ denote the associated time-dependent position operators. The symbol $\langle\ldots\rangle$ stands for a quantum ensemble average and the weighting factors Γ_{jk} have the form

$$\Gamma_{jk} = \overline{b_j}^*\,\overline{b_k} + \delta_{jk}\overline{|b_j - \overline{b_j}|^2}, \qquad (3)$$

where b_j and b_k are the (complex) scattering lengths[1,17] of the atoms j and k, respectively. For a given atom the average runs over all isotopes and combinations of the nuclear and neutron spins and we note that $b_{j,\mathrm{coh}} \equiv \overline{b_j}$ and $b_{j,\mathrm{inc}} \equiv (\overline{|b_j - \overline{b_j}|^2})^{1/2}$ are, respectively, the coherent and incoherent scattering lengths of atom j. Coherent and incoherent scattering probe, respectively, the collective and average single atom dynamics of the system under consideration, but since these scattering types are not separable without special spin-polarization experiments,[18–20] we will not explicitly distinguish between them.

The intermediate scattering function fulfills the symmetry relations of a quantum time correlation function,

$$F^*(\mathbf{q},t) = F(\mathbf{q},-t), \qquad (4)$$
$$F(\mathbf{q},-t) = F(-\mathbf{q},t+i\beta\hbar), \qquad (5)$$

where $\beta = 1/k_B T$ is the inverse Boltzmann temperature. For the dynamic structure factor Eq. (5) translates into

$$\tilde{F}(\mathbf{q},\omega) = e^{\beta\hbar\omega}\tilde{F}(-\mathbf{q},-\omega), \qquad (6)$$

which is the well-known detailed-balance relation.

B. Elastic and inelastic scattering

Noting that

$$e^{i\mathbf{q}\cdot\hat{\mathbf{R}}_j(t)} = \int d^3r\,\exp(-i\mathbf{q}\cdot\mathbf{r})\delta(\mathbf{r}-\hat{\mathbf{R}}_j(t))$$

is the spatially Fourier-transformed single particle density for atom j, we introduce the deviation of this quantity with respect to its mean value,

$$\delta\tilde{\alpha}_k(\mathbf{q},t) = e^{i\mathbf{q}\cdot\hat{\mathbf{R}}_j(t)} - \left\langle e^{i\mathbf{q}\cdot\hat{\mathbf{R}}_j(t)}\right\rangle, \qquad (7)$$

to split the intermediate scattering function into a static and a time-dependent component,

$$F(\mathbf{q},t) = F(\mathbf{q},\infty) + \delta F(\mathbf{q},t), \qquad (8)$$

which are given by

$$F(\mathbf{q},\infty) = \frac{1}{N}\sum_{j,k}\Gamma_{jk}\left\langle e^{i\mathbf{q}\cdot\hat{\mathbf{R}}_j}\right\rangle^*\left\langle e^{i\mathbf{q}\cdot\hat{\mathbf{R}}_k}\right\rangle, \qquad (9)$$

$$\delta F(\mathbf{q},t) = \frac{1}{N}\sum_{j,k}\Gamma_{jk}\left\langle \delta\tilde{\alpha}_j^\dagger(\mathbf{q},0)\delta\tilde{\alpha}_k(\mathbf{q},t)\right\rangle. \qquad (10)$$

Making the the physically reasonable assumption

$$\lim_{t\to\infty}\delta F(\mathbf{q},t) = 0, \qquad (11)$$

shows that $F(\mathbf{q},\infty)$ is the asymptotic form of the intermediate scattering function and it follows by Fourier transform of Eq. (8) that

$$\tilde{F}(\mathbf{q},\omega) = F(\mathbf{q},\infty)\delta(\omega) + \delta\tilde{F}(\mathbf{q},\omega). \qquad (12)$$

Therefore $F(\mathbf{q},\infty)$ represents the elastic amplitude of the Fourier spectrum and $\delta\tilde{F}(\mathbf{q},\omega)$ its inelastic component. Here "inelastic" is to be understood as "non-elastic" and includes also the quasielastic component of the spectrum, which is very close to the elastic line and describes relaxation and diffusion processes.

C. Generic form of the scattering functions

For modeling purposes it is convenient to introduce the normalized relaxation function

$$\phi(\mathbf{q},t) = \delta F(\mathbf{q},t)/\delta F(\mathbf{q},0), \qquad (13)$$

noting that this function does not monotonously decay for short times. This leads to the generic form

$$F(\mathbf{q},t) = F(\mathbf{q},\infty) + (F(\mathbf{q},0) - F(\mathbf{q},\infty))\phi(\mathbf{q},t) \qquad (14)$$

of the intermediate scattering function which translates into the corresponding generic form

$$\tilde{F}(\mathbf{q},\omega) = F(\mathbf{q},\infty)\delta(\omega) \\ + (F(\mathbf{q},0) - F(\mathbf{q},\infty))\tilde{\phi}(\mathbf{q},\omega) \qquad (15)$$

of the dynamic structure factor. We note that

$$F(\mathbf{q},0) = \frac{1}{N}\sum_{j,k}\Gamma_{jk}\left\langle e^{i\mathbf{q}\cdot(\hat{\mathbf{R}}_k-\hat{\mathbf{R}}_j)}\right\rangle \qquad (16)$$

is the total static structure factor, which tends for $q \equiv |\mathbf{q}| \to \infty$ to a constant value,

$$\lim_{q\to\infty}F(\mathbf{q},0) = \frac{1}{N}\sum_k\Gamma_{kk}, \qquad (17)$$

and oscillates for smaller q-values around that constant. For modeling purposes it is convenient to normalize the intermediate scattering function such that

$$\frac{1}{N}\sum_k\Gamma_{kk} = 1. \qquad (18)$$

D. Hydrogen-rich systems

We finally consider the frequent of case of neutron scattering from hydrogen-rich systems, such as proteins and

polymers. Because of the exceptionally large cross section for incoherent scattering from hydrogen, it is sufficient to consider only these atoms, setting $\Gamma_{jk} = \delta_{jk}$. With the normalization (18) it then follows that

$$F(\mathbf{q}, 0) = 1 \qquad (19)$$

and the generic form of the intermediate scattering function simplifies to

$$F(\mathbf{q}, t) = EISF(\mathbf{q}) + (1 - EISF(\mathbf{q}))\phi(\mathbf{q}, t), \qquad (20)$$

where

$$EISF(\mathbf{q}) = \frac{1}{N} \sum_{j \in \mathbb{H}} \left| \left\langle e^{i\mathbf{q} \cdot \hat{\mathbf{R}}_j} \right\rangle \right|^2 \qquad (21)$$

is referred to as Elastic Incoherent Structure Factor and the relaxation function has the form

$$\phi(\mathbf{q}, t) = \frac{\sum_{j \in \mathbb{H}} \left\langle \delta \tilde{\alpha}_j^\dagger(\mathbf{q}, 0) \delta \tilde{\alpha}_j(\mathbf{q}, t) \right\rangle}{\sum_{j \in \mathbb{H}} \left\langle \delta \tilde{\alpha}_j^\dagger(\mathbf{q}, 0) \delta \tilde{\alpha}_j(\mathbf{q}, 0) \right\rangle}. \qquad (22)$$

III. PSEUDOELASTIC SCATTERING

A. Measured and true elastic intensity

We will now consider a measured dynamic structure factor, which is always broadened due to finite instrumental resolution. Defining $\tilde{R}(\omega)$ to be the instrumental resolution function and omitting for simplicity the q-dependence of the relevant quantities, the measured dynamic structure factor is given by the frequency convolution of the true dynamic structure factor and the resolution function,

$$\tilde{F}_m(\omega) = (\tilde{R} * \tilde{F})(\omega) \equiv \int_{-\infty}^{+\infty} d\omega' \, \tilde{R}(\omega - \omega') \tilde{F}(\omega'). \quad (23)$$

With (15) we obtain then in a first step

$$\tilde{F}_m(\omega) = F(\infty)\tilde{R}(\omega) + (F(0) - F(\infty))(\tilde{R} * \tilde{\phi})(\omega). \quad (24)$$

We define now the measured elastic intensity through the integral

$$F_m(\infty) \equiv \int_{-\epsilon}^{+\epsilon} d\omega \, \tilde{F}_m(\omega), \qquad (25)$$

where $\epsilon > 0$ is defined such that

$$\int_{-\epsilon}^{+\epsilon} d\omega \, \tilde{R}(\omega) \lessapprox 1, \qquad (26)$$

and the measured total static structure factor through

$$F_m(0) \equiv \int_{\omega_{\min}}^{\omega_{\max}} d\omega \, \tilde{F}_m(\omega), \qquad (27)$$

where $[\omega_{\min}, \omega_{\max}]$ is the dynamical range of the instrument. It follows then from the generic form (24) of the measured, resolution-broadened dynamic structure factor that

$$F_m(\infty) \approx F(\infty) + (F_m(0) - F(\infty))\xi, \qquad (28)$$

where ξ is the pseudoelastic contribution due to finite instrumental resolution,

$$\xi = \int_{-\epsilon}^{+\epsilon} d\omega \, (\tilde{R} * \tilde{\phi})(\omega). \qquad (29)$$

Supposing that this contribution can be reliably computed on the basis of appropriate models for the relaxation function and the instrumental resolution, the "true" elastic intensity may be estimated through

$$F(\infty) \approx \frac{F_m(\infty) - \xi F_m(0)}{1 - \xi}. \qquad (30)$$

For essentially incoherent scattering the measured total structure factor is not needed, since one knows that the incoherent static structure factor is simply a constant. Assuming the normalization (18), one can replace $F_m(0) \to 1$ in this case. It is also worthwhile noting that the standard definition of the elastic amplitude[21,22] corresponds in our notation to the measured one.

B. Model

1. Symmetrized correlation function

The symmetry relations (4) and (5) show that the intermediate scattering function becomes a real symmetrical function in time if one considers the classical limit $\hbar \to 0$ and if one can assume that the scattering functions are invariant with respect to the parity operation $\mathbf{q} \to -\mathbf{q}$. Based on this observation, Schofield proposed to use the time-symmetrized real function $F^{(+)}(\mathbf{q}, t) \equiv F(\mathbf{q}, t - i\beta\hbar/2)$ to define the semiclassical approximation $F^{(+)}(\mathbf{q}, t) \approx F^{(cl)}(\mathbf{q}, t)$.[23] To be able to work with classical relaxation models, we consider now the time-symmetrized generic form

$$F^{(+)}(t) = F(\infty) + (F(0) - F(\infty))\phi^{(+)}(t) \qquad (31)$$

of the intermediate scattering function, where the relaxation function is defined as

$$\phi^{(+)}(t) \equiv \frac{\phi(t + i\beta\hbar/2)}{\phi(i\beta\hbar/2)}, \qquad (32)$$

in order to ensure its correct normalization.

2. "Minimalistic" model

We assume now that the symmetrized relaxation function is well represented by the model

$$\phi^{(+)}(t) = \phi_{\mathrm{ML}}(t) \qquad (33)$$

where $\phi_{\mathrm{ML}}(.)$ is the "stretched" Mittag-Leffler (ML) function,

$$\phi_{\mathrm{ML}}(t) \equiv E_\alpha(-(|t|/\tau)^\alpha) \quad (0 < \alpha \leq 1). \qquad (34)$$

The Mittag-Leffler function, $E_\alpha(z)$, is an entire function in the complex plane,[24] and the Taylor series $E_\alpha(z) = \sum_{n=0}^\infty \frac{z^n}{\Gamma(1+\alpha n)}$ shows that $E_1(z) = \exp(z)$. The most important property of the model relaxation function (34) is that it decays asymptotically with a power law,

$$\phi_{\mathrm{ML}}(t) \overset{t\to\infty}{\sim} \frac{(t/\tau)^{-\alpha}}{\Gamma(1-\alpha)}. \qquad (35)$$

Inserting (34) into the generic form (31) of the symmetrized intermediate scattering leads to the model

$$F^{(+)}(t) = F(\infty) + (F(0) - F(\infty))E_\alpha(-(|t|/\tau)^\alpha) \quad (36)$$

which has *a priori* three parameters:

1. the time scale parameter, τ,

2. the form parameter, α,

3. the plateau value $F(\infty) \equiv \lim_{t\to\infty} F^{(+)}(t)$.

In this form the model has been used in recent publications,[13–15] noting that only incoherent scattering has been considered, where $F(0) = 1$. In the following this restriction will not be made, assuming that an estimation for $F(0) \equiv F(\mathbf{q}, 0)$ can be provided according to Eq. (27).

The dynamic structure factor corresponding to the model (36) has then the form

$$S^{(+)}(\omega) = F(\infty)\delta(\omega) + (F(0) - F(\infty))\tilde{\phi}_{\mathrm{ML}}(\omega) \quad (37)$$

where the Fourier transformed relaxation function is a "generalized Lorentzian",[25]

$$\tilde{\phi}_{\mathrm{ML}}(\omega) = \frac{\sin\left(\frac{\pi\alpha}{2}\right)}{\pi\omega\left((\tau\omega)^{-\alpha} + (\tau\omega)^\alpha + 2\cos\left(\frac{\pi\alpha}{2}\right)\right)}, \quad (38)$$

which follows from the even simpler analytical form of its Laplace transform,[24]

$$\hat{\phi}_{\mathrm{ML}}(s) = \frac{1}{s(1 + (s\tau)^{-\alpha})}, \qquad (39)$$

by using the identity $\tilde{\phi}_{\mathrm{ML}}(\omega) = \Re\{\hat{\phi}_{\mathrm{ML}}(i\omega)\}$. The Fourier spectrum (38) becomes a "normal" Lorentzian function for $\alpha \to 1$.

3. Pseudoelastic model contribution

The estimation of the plateau value of a function from experimental data with an instrument-limited finite time range is clearly a delicate task and it is desirable to be to have some consistency check in which experimental data are used. This can be achieved if the pseudoelastic contribution, ξ, can be efficiently corrected for the given model relaxation function, such that the estimation (30) can be integrated into the fitting procedure. For this purpose we will assume that the resolution function is well represented by a Gaussian function,

$$\tilde{R}(\omega) = \frac{1}{\sqrt{2\pi}\sigma}e^{-\frac{\omega^2}{2\sigma^2}} \longleftrightarrow R(t) = e^{-\frac{\sigma^2 t^2}{2}}, \qquad (40)$$

where σ is approximatively the half width at half maximum (HWHM) of the instrument under consideration. Working with symmetrized neutron scattering spectra and the model relaxation function $\phi_{\mathrm{ML}}(t)$, the resulting pseudoelastic contribution becomes then a function of the parameters α, τ, and σ,

$$\xi_{\mathrm{ML}}(\tau, \alpha, \sigma) = \int_{-\epsilon}^{+\epsilon} d\omega \, (\tilde{R} * \tilde{\phi}_{\mathrm{ML}})(\omega), \qquad (41)$$

such that

$$F(\infty; \tau, \alpha, \sigma) \approx \frac{F_m(\infty) - \xi_{\mathrm{ML}}(\tau, \alpha, \sigma)F_m(0)}{1 - \xi_{\mathrm{ML}}(\tau, \alpha, \sigma)}, \qquad (42)$$

replaces the fit parameter $F(\infty)$. For a Gaussian function we have $\int_{-3\sigma}^{+3\sigma} d\omega \, \tilde{R}(\omega) \approx 0.9978$, such that $\epsilon = 3\sigma$ is a good choice.

C. Computing ξ_{ML}

In order to obtain a quasi-analytical formula for the pseudoelastic contribution ξ_{ML} defined in Eq. (41) we introduce the boxcar function

$$\tilde{W}(\omega) = \Theta\left(1 - \frac{|\omega|}{\epsilon}\right) \longleftrightarrow W(t) = \frac{2\sin(\epsilon t)}{t}, \qquad (43)$$

where $\epsilon > 0$ is the cutoff frequency. With Parseval's theorem and the convolution theorem of the Fourier transform,

$$(\tilde{R} * \tilde{\phi}_{\mathrm{ML}})(\omega) \longleftrightarrow R(t)\phi_{\mathrm{ML}}(t), \qquad (44)$$

we write in a first step

$$\xi_{\mathrm{ML}} = \int_{-\infty}^{+\infty} d\omega \, \tilde{W}(\omega)(\tilde{R} * \tilde{\phi}_{\mathrm{ML}})(\omega)$$
$$= \frac{1}{2\pi}\int_{-\infty}^{+\infty} dt \, W(t)R(t)\phi_{\mathrm{ML}}(t).$$

Defining the auxiliary function

$$H(t) \equiv W(t)R(t)\phi_{\mathrm{ML}}(t), \qquad (45)$$

and noting that all functions on the r.h.s. are even in time, it follows that

$$\xi_{ML} = \frac{1}{\pi}\int_0^\infty dt \, e^{-st}H(t)\Big|_{s=0}. \qquad (46)$$

The pseudoelastic contribution ξ_{ML} may thus be written as Laplace transform of a product of three functions, evaluated at $s = 0$. We use now that for a pair of functions, $f(t)$ et $g(t)$,

$$\int_0^\infty dt\, e^{-st} f(t) g(t) = \frac{1}{2\pi i} \oint_C ds'\, \hat{f}(s - s') \hat{g}(s'), \quad (47)$$

where C encircles all singularities of the integrand, and use this formula in two steps:

1. Compute

$$\hat{\phi}_{\mathrm{ML}}^{(R)}(s) = \frac{1}{2\pi i} \oint_C ds'\, \hat{\phi}_{\mathrm{ML}}(s - s') \hat{R}(s'), \quad (48)$$

2. Compute

$$\xi_{ML} = \frac{1}{\pi} \left\{ \frac{1}{2\pi i} \oint_C ds'\, \hat{\phi}_{\mathrm{ML}}^{(R)}(-s') \hat{W}(s') \right\}. \quad (49)$$

Here an analytical form is known for the Laplace transformed model relaxation function, $\hat{\phi}_{\mathrm{ML}}(s)$, (see Eq. (39)), for the Laplace transform of the model resolution time window,

$$\hat{R}(s) = \frac{1}{\sigma} \sqrt{\frac{\pi}{2}} e^{\frac{s^2}{2\sigma^2}} \mathrm{erfc} \left(\frac{s}{\sqrt{2}\sigma} \right), \quad (50)$$

and for the Laplace transform of $W(t)$,

$$\hat{W}(s) = 2\,\mathrm{arccot} \left(\frac{s}{\epsilon} \right). \quad (51)$$

An analytical form of the contour integrals (48) and 49) cannot be found, but a good quasi-analytical approximation can be obtained by replacing $\hat{R}(s)$ and $\hat{W}(s)$ by Padé approximants,[26]

$$\hat{R}(s) \approx \frac{1}{\sigma} \frac{P(s/\sigma)}{Q(s/\sigma)}, \quad (52)$$

$$\hat{W}(s) \approx \frac{P'(s/\epsilon)}{Q'(s/\epsilon)}, \quad (53)$$

where $P(.), Q(.), P'(.), Q'(.)$ are polynomials. We note here that the method has been recently used to compute a good approximation for the resolution-broadened Fourier transform $\tilde{\phi}_{\mathrm{ML}}^{(R)}(\omega)$.[14] Introducing appropriately scaled integration variables, the contour integrals (48) and 49) may then be evaluated by the residue theorem of complex analysis. The details are described in Appendix A and the result is

$$\xi_{\mathrm{ML}} \approx \frac{1}{\pi} \sum_{j=1}^m \sum_{k=1}^{m'} \chi \lambda c_j d_k \hat{\Phi}_{\mathrm{ML}} \left(-\chi \left(u_j + \lambda v_k \right) \right), \quad (54)$$

where $\hat{\Phi}_{\mathrm{ML}}(.)$ is the scale-free version of the Laplace-transformed relaxation function $\hat{\phi}_{\mathrm{ML}}(.)$,

$$\hat{\Phi}_{\mathrm{ML}}(u) = \frac{1}{u(1 + u^{-\alpha})}, \quad (55)$$

χ and λ are the dimensionless scaling parameters

$$\chi = \sigma\tau \quad \text{and} \quad \lambda = \frac{\epsilon}{\sigma}, \quad (56)$$

and $\{u_j\}$ and $\{v_k\}$ are the roots of the polynomials $Q(u)$ and $Q'(v)$, respectively. The coefficients

$$c_j = \frac{P(u_j)}{\Pi_{k=1, k\neq j}^m \left(u_j - u_k \right)}, \quad (57)$$

$$d_k = \frac{P'(v_k)}{\Pi_{l=1, l\neq k}^{m'} \left(v_k - v_l \right)}, \quad (58)$$

are the residues of the dimensionless expressions $P(u)/Q(u)$ and $P'(v)/Q'(v)$, evaluated at the respective roots of the denominator polynomials. We have thus $Q(u_j) = 0$ and $Q'(v_k) = 0$. The final expression (54) for ξ_{ML} is thus the linear superposition of simple terms of the form (55). Coding ξ_{ML} as a compiled function leads to sufficiently short execution times which allow for integrating this function into a fitting procedure.

D. Numerical test

To obtain a systematic picture of the pseudoelastic contribution as a function of τ and α, we compute it according to Eq. (54) for $\alpha = k \times 0.1$, $k = 0, \ldots, 10$. In view of later applications we define σ to be resolution (HWHM) of the IN16B spectrometer, $\sigma = 1.75\,\mu eV$, and we set $\epsilon = 3\sigma$. We vary then $\chi \in [\sigma\tau_{\min}, \sigma\tau_{\max}]$, where $\tau_{\min} = 0.1$ ps and $\tau_{\max} = 10^4$ ps (solid lines). For comparison we compute ξ_{ML} by numerical integration of $\phi_{\mathrm{ML}}^{(R)}(\omega)$, choosing the same values for α, σ, and ϵ and fixing τ to the discrete values $\tau = 10^j$ ps, $j = -1, \ldots, 4$ (points). Defining the matrices $\boldsymbol{\xi}_{\mathrm{ML}} \equiv (\xi_{\mathrm{ML}}[j, k])$ and $\boldsymbol{\xi}_{\mathrm{ML}}^{(\mathrm{n. i.})} \equiv (\xi_{\mathrm{ML}}^{(\mathrm{n. i.})}[j, k])$, where "n.i." stands for "numerical integration", we find that

$$\|\boldsymbol{\xi}_{\mathrm{ML}}^{(\mathrm{n. i.})} - \boldsymbol{\xi}_{\mathrm{ML}}\| = 3.45 \times 10^{-6},$$

where $\| \ldots \|$ is defined as maximum singular value of the difference matrix. The results of the calculations are shown in Fig. 1. On observes that for "good resolutions", where $\sigma\tau < 1$, the pseudoelastic contributions increases with decreasing α, and the opposite is true for "bad resolutions", where $\sigma\tau > 1$. We note that $\lim_{\alpha \to 0} \phi_{\mathrm{ML}}(t) = 1/2$ for any $t > 0$, which explains the results for $\alpha = 0$. All calculations have been performed with Padé-approximations of order $m = 8$ for the denominator polynomials $Q(u)$ and $Q'(u)$ and order $n = 8$ for the corresponding numerator polynomials, $P(u)$ and $P'(u)$, choosing $s = 1$ as reference point. Constructing the Padé-approximant for the resolution function through

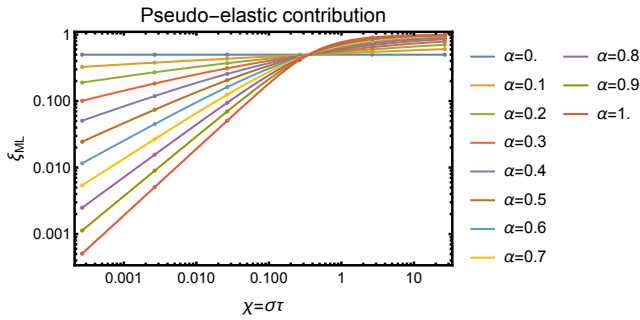$$\tilde{R}_{\mathrm{Padé}}(\omega) \equiv \frac{1}{\pi} \Re \left\{ \frac{P(i\omega)}{Q(i\omega)} \right\}$$

FIG. 1: Pseudoelastic contribution ξ_{ML} as a function of $\chi \equiv \sigma\tau$ and α. The solid lines correspond to the calculation according to Eq. (54) and the points to control calculations by numerical integration. More explanations are given in the text.

we find that

$$|\tilde{R}_{\mathrm{Pad\acute{e}}}(\omega) - \tilde{R}(\omega)| < 10^{-6}$$

in the relevant ω-domain. All computations have been performed with the Wolfram Mathematica software.[27]

IV. APPLICATIONS

A. QENS analysis of Myelin Basic Protein

To illustrate the pseudoelastic contribution to elastic scattering we consider now a concrete example related to a recently published QENS study of Myelin Basic Protein (MBP) in aqueous solution.[15] Myelin Basic Protein is an elementary constituent of the myelin sheath of nerves and in aqueous solution it is an intrinsically disordered protein (IDP). The incoherent QENS spectra for the study cited above have been recorded on the new IN16B spectrometer of the Institut Laue-Langevin, using the BATS option (Backscattering And Time-of-flight Spectrometer) with an instrumental resolution (FWHM) of 3.5 μeV. The translational diffusion constant, D, of MBP was measured separately by dynamic light scattering (DLS) and was then injected into the fit, writing $F^{(+)}(q,t) = \exp(-Dq^2|t|)F_{\mathrm{int}}^{(+)}(q,t)$, where $F_{\mathrm{int}}^{(+)}(q,t)$ is the symmetrized intermediate scattering function for internal motions, the generic form of which is given by Eq. (36). The implicit assumption is here that global and internal motions are not correlated. As mentioned in Ref. [15], the resulting fits for $EISF$, α, and τ vary only little if the diffusion constant is simply neglected. This is illustrated in Fig. 2, which shows a log-log plot of the Fourier spectrum of the fitted model relaxation function for MBP in D_2O buffer ($T = 283$ K, $q = 1.2/\text{Å}$) for the dynamical range of the instrument, together with the corresponding diffusion-broadened counterpart resulting from the damping factor $\exp(-Dq^2|t|)$ of the intermediate scattering function. We
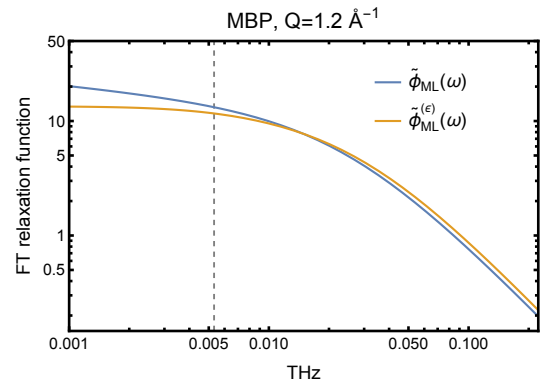

FIG. 2: Impact of global diffusion on the Fourier spectrum of the model relaxation function for MBP in D_2O buffer at $T = 283$ K and $q = 1.2/\text{Å}$. The solid blue line labels the relaxation function and the yellow line the corresponding function with the diffusion damping factor, where $D = 3.3\,\text{Å}^2/\text{ns}$ from DLS. The vertical dashed indicates the instrumental resolution (FWHM).

take here $D = 3.3\,\text{Å}^2/\text{ns}$ from DLS. Having this figure in mind, the resolution-deconvolved intermediate scattering function can therefore be fitted directly with the model (36). It is worthwhile mentiong that a more sophisticated treatment of global protein motions, including rotational diffusion,[28–31] would be needed for the analysis of QENS data with even higher ω-resolution, but are fortunately not necessary here, noting that rotational and and translational degrees of freedom in MBP are difficult to disentangle.

The impact of pseudoelastic scattering on the observed elastic intensities is illustrated in Fig. 3, which shows again the Fourier spectrum of the fitted model relaxation function $\tilde{\phi}_{\mathrm{ML}}(\omega)$ for the same parameters as in Fig. 2 (blue line), together with the model resolution function (yellow line), where the instrumental resolution (HWHM) corresponds to $\sigma = 0.0027$ THz, and the resulting resolution-broadened spectrum, $\tilde{\phi}_{\mathrm{ML}}^{(R)}(\omega)$ (red line). The (dimensionless) area in light red is the corresponding pseudoelastic contribution, which is for this example $\xi_{\mathrm{ML}} \approx 0.47$ with $\epsilon = 3\sigma$. The difference between the model spectrum and its resolution-broadened version should also be noticed.

An important result of the study in Ref. [15] was that the fitted EISF vanishes. This can be explained by the fact that MBP in solution is a very flexible molecule, such that $\langle \exp(i\mathbf{q} \cdot \hat{\mathbf{R}}_j) \rangle \approx 0$. In the Gaussian approximation[32,33] (in $q \equiv |\mathbf{q}|$) of the elastic amplitude one would write

$$EISF(\mathbf{q}) \overset{|\mathbf{q}| \to 0}{\sim} \frac{1}{N} \sum_{j \in \mathbb{H}} e^{-\frac{1}{3}|\mathbf{q}|^2 \langle \hat{\mathbf{u}}_j^2 \rangle} \approx 0, \qquad (59)$$

where $\langle \hat{\mathbf{u}}_j^2 \rangle \equiv \langle (\hat{\mathbf{R}}_j - \langle \hat{\mathbf{R}}_j \rangle)^2 \rangle$ is the mean square position fluctuation of (hydrogen) atom j. For smaller q-values a vanishing EISF stands thus for large motional amplitudes
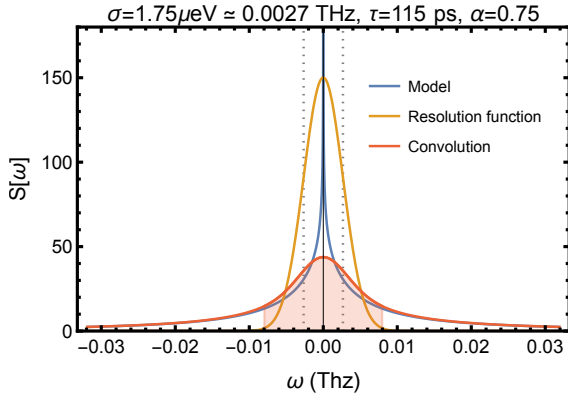
FIG. 3: Model relaxation function $\tilde{\phi}_{\mathrm{ML}}(\omega)$ (blue line), model resolution function (yellow line) and the resulting convolution $\tilde{\phi}_{\mathrm{ML}}^{(R)}(\omega)$ (red line) for the resolution of the IN16B spectrometer at ILL. The values for τ and α are taken from the fit parameters shown in Fig. 4 (three-parameter fit for $|\mathbf{q}| = 0.8/\mathrm{Å}^{-1}$). The vertical dotted lines indicate the instrumental resolution and the light red area corresponds to the pseudoelastic contribution of $\xi_{\mathrm{ML}} \approx 0.47$ for this example.

of the atoms. Keeping in mind that the EISF is a "theoretical quantity", $EISF(\mathbf{q}) = F_{\mathrm{inc}}(\mathbf{q}, \infty)$, which can only be determined by assuming a model, we can now check the fits of the three-parameter model (36) with a two-parameter fit, where the EISF is eliminated according to Eq. (27). The results in Fig. 4 show that α and τ change only slightly comparing the two- and three-parameter fits and in particular that the vanishing EISF from the three-parameter fits is confirmed if one considers the relevant scale for this quantity. This means that the measured elastic intensity (bottom panel, green points) is entirely due to the "pseudoelastic contribution" defined through Eq. (54). For its calculation we used the same Padé approximations as for the numerical test described in Section III D. We note here that the standard estimation of the parameter errors for the three-parameter fits (yellow dots) leads to error bars which are sometimes hardly visible in the plots and cannot be performed for the two-parameter fits. The reason is purely technical – namely that in the latter case the EISF "parameter" is a compiled function which is passed as an argument to the fit routine of the Mathematica software.[27] Concerning this point, we think that the error of fit parameters is anyway better estimated by comparing the results of the three- and two-parameter fits.

B. QENS analysis of Myoglobin

To show that the model (36) does not systematically lead to vanishing EISFs for proteins in solution, we have analyzed QENS data from apo-myoglobin at $T = 284$ K in D_2O buffer (pD = 6), which have been recorded on the IN5 spectrometer at the Institut Laue-Langevin in Grenoble, at a resolution (FWHM) of $11.6\,\mu eV$.[34] In
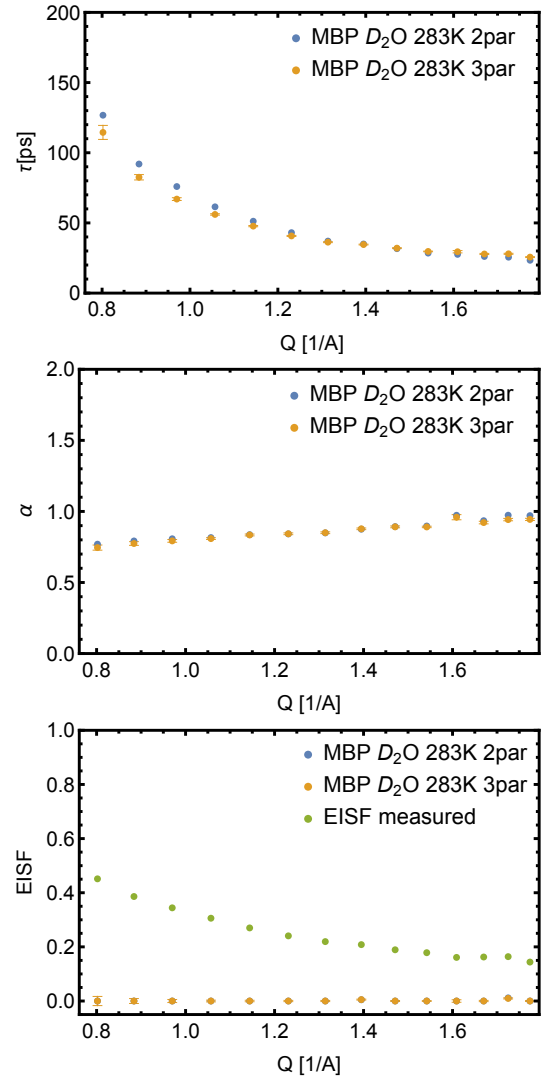

FIG. 4: From top to bottom: Characteristic time scale, τ, form parameter, α, and elastic scattering amplitude, $EISF$, for incoherent QENS from MBP in solution. Blue dots correspond to a two-parameter fit, where $EISF \equiv EISF(\tau, \alpha, \sigma)$ according to Eq. (42) and yellow points to a three-parameter fit. Concerning the EISF, the green points correspond to the measured elastic intensity $F_m(\infty) \equiv F_m(\mathbf{q}, \infty)$ defined in Eq. (25) and on the scale of the plot the results two- and three-parameter plots are indistinguishable.

contrast to MBP, myoglobin is a compactly folded globular protein of about the same weight, but with a well-defined three-dimensional structure containing eight α-helices as secondary structure elements. Fig. 5 shows that here, as for MBP, global diffusion can be neglected for the analysis of the QENS spectra. We insert here a global diffusion coefficient of $D = 10.1\,\mathrm{Å}^2/\mathrm{ns}$, which is the mean of the values reported in Refs. [35] and [36], respectively, but the exact value is here not important. We note in this context that a somewhat smaller value of $D \approx 8\,\mathrm{Å}^2/\mathrm{ns}$ is obtained by a very rough estimation
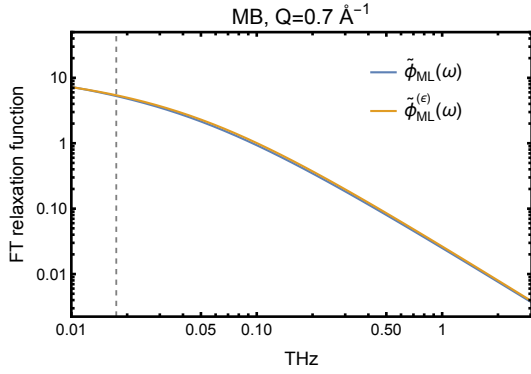
FIG. 5: Impact of global diffusion on the model dynamic structure factor at $q = 0.7/\text{Å}$ for myoglobin in solution. The legends are the same as in Fig. 2.

from the Stokes-Einstein relation, $D = k_B T/6\pi\eta R_h$, inserting here a hydrodynamic radius of $R_h = 2\,\text{nm}$ for a myoglobin molecule and for η the kinematic viscosity of water at $284\,\text{K}$ ($\eta = 1.306\,\text{mPa s}$).[37] The hydrodynamic radius is here calculated from PDB structure 1BVC for apo-myoglobin, assuming the latter to be a sphere.

Since the impact of global diffusion can be neglected, model (36) has again be fitted directly to the resolution-deconvolved intermediate scattering function. Fig. 6, bottom panel, shows that the EISF for myoglobin is clearly non-vanishing and that both the three- and the two-parameter fits give again similar results. The fact that the atomic motions in a globular, compactly folded protein are more hindered than in a polymer-like intrinsically disordered protein like MBP is thus clearly reflected in the corresponding EISFs, and it should be noted that this effect is much more pronounced for the resolution-corrected elastic intensities than for the measured ones. It should also be noted that both the characteristic time scale, τ, and the form parameter, α, are systematically smaller for myoglobin, reflecting more hindered localized motions of the atoms in this more compactly folded protein.

C. Resolution correction for $\langle \hat{\mathbf{u}}^2 \rangle$

The Gaussian approximation (59) of the EISF is also known as Debye-Waller factor and has been used for decades to analyse "elastic scans" of incoherent neutron scattering from D_2O-hydrated protein powders in the low q-region, in order to infer the average mean square position fluctuations of the (hydrogen) atoms in the protein from these data. There is a large bulk of literature on that subject and we cite here only Refs. [7,38,39]. It follows then from Eqs. (30) and Eq. (59) that the "true", resolution-corrected mean square position fluctuation, averaged over all atoms, is given by

$$\overline{\langle \hat{\mathbf{u}}^2 \rangle} \overset{q\to 0}{\approx} -\frac{3}{q^2} \log\left(\frac{EISF_m(q) - \xi(q)}{1 - \xi(q)} \right). \quad (60)$$
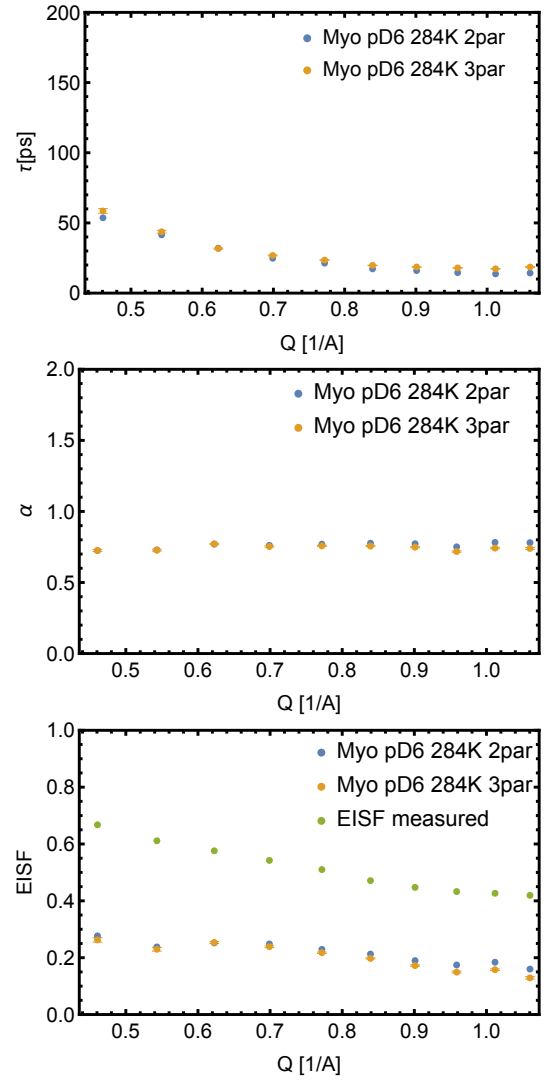

FIG. 6: The same quantities as in Fig. 6 for myoglobin in solution. More details are given in the text.

We assume here an isotropic sample and indicate explicitly the dependency of all involved quantities on $q \equiv |\mathbf{q}|$. Writing $EISF_m(q) = \exp(-q^2 \overline{\langle \hat{\mathbf{u}}^2 \rangle}_m/3)$ and developing Expression (60) into a power series in $\xi(q)$ we obtain

$$\overline{\langle \hat{\mathbf{u}}^2 \rangle} \approx \overline{\langle \hat{\mathbf{u}}^2 \rangle}_m + \sum_{n=1}^{\infty} \frac{3}{nq^2} \left(e^{\frac{n}{3} q^2 \overline{\langle \hat{\mathbf{u}}^2 \rangle}_m} - 1 \right) \xi(q)^n$$

$$\overset{q\to 0}{\approx} \overline{\langle \hat{\mathbf{u}}^2 \rangle}_m \sum_{n=0}^{\infty} \xi(q)^n,$$

where the geometrical series can be summed up to give

$$\overline{\langle \hat{\mathbf{u}}^2 \rangle} \overset{q\to 0}{\approx} \frac{\overline{\langle \hat{\mathbf{u}}^2 \rangle}_m}{1 - \xi(q)}. \quad (61)$$

Fig. 7 shows the correction factor $1/(1-\xi)$ which needs to be applied to obtain the "true", resolution-corrected
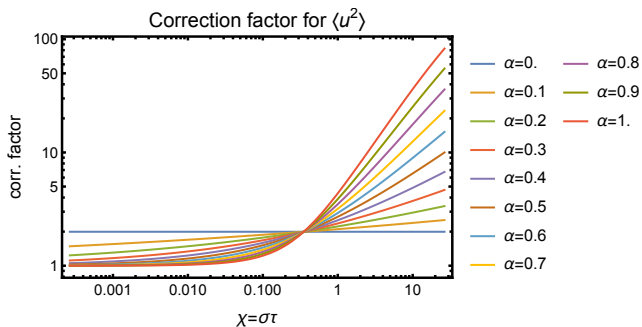
FIG. 7: Correction factor to convert the measured mean square position fluctuations into the resolution-corrected ones. More explanations are given in the text.

mean square position fluctuations from the measured ones. At a first glance, the large correction factors for "bad resolutions" and close to exponential relaxation may surprise, but they can be understood noting that in this case an elastic scan contains practically the whole integral over the quasielastic line such that $\xi \lessgtr 1$.

V. CONCLUSIONS AND DISCUSSION

In the paper we have presented a quasi-analytical method for computing the pseudoelastic contribution of quasielastic scattering to the elastic neutron scattering amplitude, which enables the estimation of the true elastic scattering amplitude for the Mittag-Leffler relaxation model. Due to the computational efficiency of the method, which is based on Padé approximants for the Laplace transformed relaxation and resolution functions, the true elastic scattering amplitude can be eliminated in the model (36) by using the measured elastic intensity and the two parameters α and τ of the ML relaxation function together with the instrument resolution, σ, as input. We have applied the method to confirm the results of a recent analysis of incoherent QENS spectra from the internal dynamics of Myelin Basic Protein in solution,[15] which revealed in particular a vanishing EISF. MBP is an intrinsically disordered protein and to demonstrate that the vanishing EISF is the result of its "floppiness" and the corresponding large motional amplitudes of the atoms, we performed a comparative study for myoglobin in solution. Myoglobin has about the same weight as MBP, but in contrast to the latter it is a globular protein with a well defined structure. As one would expect, we find here a clearly non-vanishing EISF as a result of the more hindered atomic motions in a compactly folded protein. An important result in this context is that the resolution-corrected EISF shows this result much more clearly than the measured one. We have also shown that the resolution corrections of the elastic intensity may also strongly impact atomic mean square position fluctuations which are routinely extracted from so-called elastic scans.

It should be mentioned again that the elastic intensity is a "theoretical quantity", which can only be extracted from experimental QENS spectra by assuming a model for the relaxation dynamics of the protein under consideration. In that light, our analysis is a consistency check for the the ML relaxation model which does in principle not exclude other models for the relaxation function. There is, however, a good reason to use the ML relaxation function whenever the relaxation function is supposed to have the asymptotic power law form (35) and the transition from short-time ballistic motion to the asymptotic dynamics cannot be resolved on the instrument under consideration.

The ML relaxation function has the remarkable property of being "weakly self-similar"[40] for every $t > 0$ and the physical and mathematical reasons for its "universal" validity as relaxation function are developed in Ref. [41]. We resume here the essential points. From a mathematical point of view the ML relaxation function verifies an integro-differential equation of the form[24,42]

$$\partial_t \phi_{\mathrm{ML}}(t) + \tau^{-\alpha} \underbrace{\frac{d}{dt} \int_0^t dt' \frac{(t-t')^{\alpha-1}}{\Gamma(\alpha)} \phi_{\mathrm{ML}}(t')}_{\partial_t^{1-\alpha} \phi_{\mathrm{ML}}(t)} = 0, \quad (62)$$

where $\partial_t^{1-\alpha}$ denotes a fractional derivative[43] of order $1 - \alpha$. From a physical point if view Eq. (62) can be considered as a special form of the general equation of motion

$$\partial_t \phi^{(+)}(t) + \int_0^t dt' \, \kappa^{(+)}(t-t') \phi^{(+)}(t') = 0, \quad (63)$$

that any symmetric time correlation function fulfills according to the Mori-Zwanzig theory of the Generalized Langevin equation.[44–46] Here $\kappa^{(+)}(t)$ the associated memory kernel, which is itself a time autocorrelation function that can be formally derived from first principles. The only point that matters here is to consider that $\kappa^{(+)}(t)$ has two characteristic time scales, τ and τ^*, where τ characterizes the asymptotic regime of the correlation function $\phi^{(+)}(t)$ and τ^* the transition to that regime. In Ref. [41] it is then shown that the ML relaxation function emerges whenever $\tau^* \ll \tau$. In that light the fractional derivative thus represents the asymptotic form of a memory kernel.

Another point that merits some discussion is the q-dependence of τ and α that can be understood on physical grounds and that influences the pseudoelastic contribution to the elastic scattering. The decrease of τ with q simply reflects the general observation that more localized motions in proteins, resulting for instance from side-chains, are faster than those involving many atoms, such as large conformational rearrangements. The observation that α increases instead with q can be explained by the fact that descreasing q corresponds to decrease the spatial resolution, mixing in more and more slow modes, and the increasingly non-exponential character of the relaxation function is reflected in a decrease of α with q.

In a compact protein, like myoglobin, where the modes describing the internal relaxation dynamics are strongly coupled, this effect is less pronounced than in a polymer-like protein like MBP, where local entities diffuse almost independently. It should be noted that in the latter case $\alpha \approx 1$ for higher q-values.

We finally emphasize that our method is prepared to deal with coherent scattering in general. This aspect is for instance important for the increasing number of QENS studies of proteins in deuterated aqueous solutions (D_2O-buffer), where coherent scattering from the solvent becomes visible at higher momentum transfers $\gtrsim 1.5/\text{Å}$.

Appendix A: Derivation of Expression (54)

We start from eq. (48) and insert Expression (52) for the Padé approximation of the Laplace transformed instrumental time window. In addition we use that

$$\hat{\phi}_{\text{ML}}(s) = \tau \hat{\Phi}_{\text{ML}}(s\tau)$$

to obtain in a first step

$$\hat{\phi}_{\text{ML}}^{(R)}(s) = \frac{1}{2\pi i} \oint_C \frac{ds'}{\sigma} \hat{\phi}_{\text{ML}}(s-s') \frac{P(s'/\sigma)}{Q(s'/\sigma)}$$
$$\stackrel{s'/\sigma \to u}{=} \frac{1}{2\pi i} \oint_C du\, \tau \hat{\Phi}_{\text{ML}}(\tau(s-\sigma u)) \frac{P(u)}{Q(u)}$$
$$= \frac{1}{\sigma} \left\{ \frac{1}{2\pi i} \oint_C du\, \chi \hat{\Phi}_{\text{ML}} \left(\chi \left(\frac{s}{\sigma} - u \right) \right) \frac{P(u)}{Q(u)} \right\}.$$

Writing $Q(u) = \Pi_{k=1}^m (u - u_k)$ and defining the coefficients

$$c_j = \frac{P(u_j)}{\Pi_{k=1, k \neq j}^m (u_j - u_k)}$$

it follows then from the residue theorem of complex analysis that

$$\hat{\phi}_{\text{ML}}^{(R)}(s) = \frac{1}{\sigma} \sum_{j=1}^m \chi c_j \hat{\Phi} \left(\chi \left(\frac{s}{\sigma} - u_j \right) \right). \qquad \text{(A1)}$$

This expression is now inserted into the contour integral (49), and appropriate changes of the integation variables lead to

$$\xi_{ML} = \frac{1}{\pi} \left\{ \frac{1}{2\pi i} \oint_C ds' \right.$$
$$\left. \left\{ \frac{1}{\sigma} \sum_{j=1}^m \chi c_j \hat{\Phi} \left(\chi \left(-\frac{s'}{\sigma} - u_j \right) \right) \right\} \frac{P'(s'/\epsilon)}{Q'(s'/\epsilon)} \right\}$$
$$\stackrel{s'/\sigma \to u}{=} \frac{1}{\pi} \left\{ \frac{1}{2\pi i} \oint_C du \right.$$
$$\left. \left\{ \sum_{j=1}^m \chi c_j \hat{\Phi} \left(\chi \left(-u - u_j \right) \right) \right\} \frac{P'(u\sigma/\epsilon)}{Q'(u\sigma/\epsilon)} \right\}$$
$$\stackrel{\epsilon/\sigma \to \lambda, u/\lambda \to v}{=} \frac{1}{\pi} \left\{ \frac{1}{2\pi i} \oint_C dv \right.$$
$$\left. \left\{ \sum_{j=1}^m \lambda \chi c_j \hat{\Phi} \left(\chi \left(-\lambda v - u_j \right) \right) \right\} \frac{P'(v)}{Q'(v)} \right\}.$$

Writing $Q'(v) = \Pi_{l=1}^{m'} (v - v_l)$ and defining the coefficients

$$d_k = \frac{P(u_k)}{\Pi_{l=1, l \neq k}^{m'} (v_k - v_l)},$$

we get again from the residue theorem the final result

$$\xi_{\text{ML}} = \frac{1}{\pi} \sum_{j=1}^m \sum_{k=1}^{m'} \lambda \chi c_j d_k \hat{\Phi} \left(-\chi \left(u_j + \lambda v_k \right) \right), \qquad \text{(A2)}$$

where $\chi \equiv \sigma\tau$ and $\lambda \equiv \epsilon/\sigma$.

ACKNOWLEDGEMENTS

[1] S. Lovesey, *Theory of Neutron Scattering from Condensed Matter*, vol. I (Clarendon Press, Oxford, 1984).

[2] J. Fitter, T. Gutberlet, and J. Katsaras, eds., *Neutron Scattering in Biology: Techniques and Applications* (Springer, Berlin ; New York, 2006), chap. 15 and 16, Biological and Medical Physics, Biomedical Engineering, ISBN 978-3-540-29108-4.

[3] V. G. Sakai and A. Arbe, Current Opinion in Colloid & Interface Science **14**, 381 (2009), ISSN 13590294.

[4] J. Colmenero and A. Arbe, Journal of Polymer Science - Part B: Polymer Physics **51**, 87 (2013).

[5] R. Ashkar, H. Z. Bilheux, H. Bordallo, R. Briber, D. J. E. Callaway, X. Cheng, X.-Q. Chu, J. E. Curtis, M. Dadmun, P. Fenimore, et al., Acta Crystallographica Section D Structural Biology **74**, 1129 (2018), ISSN 2059-7983.

[6] J. C. Smith, P. Tan, L. Petridis, and L. Hong, Annual Review of Biophysics **47**, 335 (2018), ISSN 1936-122X, 1936-1238.

[7] W. Doster, S. Cusack, and W. Petry, Nature **337**, 754 (1989).

[8] I. Iben, D. Braunstein, W. Doster, H. Frauenfelder, M. Hong, J. Johnson, S. Luck, P. Ormos, A. Schulte, P. Steinbach, et al., Phys Rev Lett **62**, 1916 (1989).

[9] H. Frauenfelder, S. G. Sligar, and P. G. Wolynes, Science **254**, 1598 (1991).

[10] P. W. Fenimore, H. Frauenfelder, B. H. McMahon, and F. G. Parak, Proceedings of the National Academy of Sciences **99**, 16047 (2002), ISSN 0027-8424, 1091-6490.

[11] G. R. Kneller and V. Calandrini, J Chem Phys **126**, 125107 (2007).

[12] G. R. Kneller, Proceedings of the National Academy of Sciences USA **115**, 9450 (2018).

[13] M. Saouessi, J. Peters, and G. R. Kneller, The Journal of Chemical Physics **150**, 161104 (2019), ISSN 0021-9606, 1089-7690.

[14] M. Saouessi, J. Peters, and G. R. Kneller, The Journal of Chemical Physics **151**, 125103 (2019), ISSN 0021-9606, 1089-7690.

[15] A. N. Hassani, L. Haris, M. Appel, T. Seydel, A. M. Stadler, and G. R. Kneller, The Journal of Chemical Physics **156**, 025102 (2022), ISSN 0021-9606, 1089-7690.

[16] M. H. Petersen, N. Vernet, W. P. Gates, F. J. Villacorta, S. Ohira-Kawamura, Y. Kawakita, M. Arai, G. Kneller, and H. N. Bordallo, J. Phys. Chem. C p. Online preview (2021), ISSN 1932-7447, 1932-7455.

[17] M. Bée, *Quasielastic Neutron Scattering: Principles and Applications in Solid State Chemistry, Biology and Materials Science* (Adam Hilger, Bristol, 1988).

[18] P. Gerlach, O. Schärpf, W. Prandl, and B. Dorner, Le Journal de Physique Colloques **43**, C7 (1982), ISSN 0449-1947.

[19] A. M. Gaspar, S. Busch, M.-S. Appavou, W. Haeussler, R. Georgii, Y. Su, and W. Doster, Biochimica et Biophysica Acta (BBA) - Proteins and Proteomics **1804**, 76 (2010), ISSN 15709639.

[20] T. Burankova, R. Hempelmann, A. Wildes, and J. P. Embs, The Journal of Physical Chemistry B **118**, 14452 (2014), ISSN 1520-6106, 1520-5207.

[21] J. Fitter, T. Gutberlet, and J. Katsaras, eds., *Neutron Scattering in Biology: Techniques and Applications* (Springer, Berlin ; New York, 2006), chap. 15, Biological

and Medical Physics, Biomedical Engineering, ISBN 978-3-540-29108-4.

[22] Q. Berrod, K. Lagrené, J. Ollivier, and J.-M. Zanotti, EPJ Web of Conferences **188**, 05001 (2018), ISSN 2100-014X.

[23] P. Schofield, Physical Review Letters **4**, 239 (1960), ISSN 0031-9007.

[24] R. Gorenflo, A. A. Kilbas, F. Mainardi, and S. V. Rogosin, eds., *Mittag-Leffler Functions, Related Topics and Applications*, Springer Monographs in Mathematics (Springer, Heidelberg, 2014), ISBN 978-3-662-43929-6 978-3-662-43930-2.

[25] G. R. Kneller, Phys Chem Chem Phys **7**, 2641 (2005).

[26] F. W. J. Olver, D. W. Lozier, and R. F. Boisvert, *NIST Handbook of Mathematical Functions* (Cambridge Univ Pr, 2010), ISBN 978-0-521-14063-8.

[27] Wolfram Research, Inc, *Mathematica, Version 13.0*, Champaign, IL, 2019.

[28] J. Pérez, J.-M. Zanotti, and D. Durand, Biophysical Journal **77**, 454 (1999), URL https://doi.org/10.1016%2Fs0006-3495%2899%2976903-1.

[29] A. Stadler, I. Digel, G. Artmann, J. Embs, G. Zaccai, and G. Büldt, Biophysical Journal **95**, 5449 (2008), ISSN 00063495.

[30] F. Roosen-Runge, M. Hennig, F. Zhang, R. M. J. Jacobs, M. Sztucki, H. Schober, T. Seydel, and F. Schreiber, Proceedings of the National Academy of Sciences **108**, 11815 (2011), ISSN 0027-8424, 1091-6490.

[31] M. Grimaldo, F. Roosen-Runge, F. Zhang, F. Schreiber, and T. Seydel, Quarterly Reviews of Biophysics **52**, e7 (2019), ISSN 0033-5835, 1469-8994.

[32] A. Rahman, K. S. Singwi, and A. Sjölander, Physical Review **126**, 986 (1962), ISSN 0031-899X.

[33] G. R. Kneller, The Journal of Chemical Physics **145**, 044103 (2016), ISSN 0021-9606, 1089-7690.

[34] A. M. Stadler, F. Demmel, J. Ollivier, and T. Seydel, Phys. Chem. Chem. Phys. **18**, 21527 (2016), ISSN 1463-9076, 1463-9084.

[35] V. Riveros-Moreno and J. B. Wittenberg, Journal of Biological Chemistry **247**, 895 (1972), ISSN 00219258.

[36] M. Rocco and O. Byron, European Biophysics Journal **44**, 417 (2015), ISSN 0175-7571, 1432-1017.

[37] M. L. Huber, R. A. Perkins, A. Laesecke, D. G. Friend, J. V. Sengers, M. J. Assael, I. N. Metaxa, E. Vogel, R. Mareš, and K. Miyagawa, Journal of Physical and Chemical Reference Data **38**, 101 (2009), ISSN 0047-2689, 1529-7845.

[38] G. Zaccai, Science **288**, 1604 (2000).

[39] J. Fitter, T. Gutberlet, and J. Katsaras, eds., *Neutron Scattering in Biology: Techniques and Applications* (Springer, Berlin ; New York, 2006), chap. 18, Biological and Medical Physics, Biomedical Engineering, ISBN 978-3-540-29108-4.

[40] G. R. Kneller and M. Saouessi, Journal of Physics A: Mathematical and Theoretical **53**, 1 (2020).

[41] G. R. Kneller and M. Saouessi, Acta Physica Polonica B **53**, A (2022).

[42] W. Glöckle and T. Nonnenmacher, Biophysical Journal **68**, 46 (1995).

[43] K. Oldham and J. Spanier, *The Fractional Calculus* (Academic Press, New York, London, 1974).

[44] R. Zwanzig, *Statistical mechanics of irreversibility* (Wiley-

Interscience, New York, 1961), pp. 106–141, Lectures in Theoretical Physics.

[45] H. Mori, Progress of theoretical physics (1965).

[46] R. Zwanzig, *Nonequilibrium statistical mechanics* (Oxford University Press, 2001).